Electronic supplementary information:

High specific detection and near-infrared photothermal therapy of lung cancer cells with high SERS active aptamer-silver-gold shell-core nanostructures

Ping Wu, Yang Gao, Yimei Lu, Hui Zhang, and Chenxin Cai*

Jiangsu Key Laboratory of New Power Batteries, College of Chemistry and Materials Science, Nanjing Normal University, Nanjing 210097, P.R. China.

* Corresponding author, E-mail: cxcai@njnu.edu.cn (C. Cai)

MTT assay

MTT (3-(4,5-dimethyl-2-thiazolyl)-2,5-diphenyl-2H-tetrazolium bromide) assay, was used for evaluating the cell viability during the photothermal therapy. The colorimetric test assesses cell metabolic activity on the basis of the ability of the mitochondrial succinate-tetrazolium reductase system to convert the yellow dye (MTT) to a purple-colored formazan in living cells. The metabolic activity of the cell is proportional to the color density formed. For this purpose, A549 cells were seeded in 96-well plates (well diameter 6.4 mm) with a density of ~1×10^5 cells $well^{-1}$. After the cells were incubated with aptamer-Ag-Au nanostructures and irradiated with laser at 808 nm, 10 μL of MTT (Sigma) solution (5 mg mL^{-1} in PBS, pH 7.4) was added into each well and incubated for 4 h at 37 °C. During the incubation, MTT (a yellow tetrazole) was reduced to insoluble purple formazan by mitochondrial reductase in living cells. Afterward, the product was dissolved with 100 μL of dimethylsulfoxide (DMSO). Absorbance was recorded at 550 nm on a Synergy 2 microplate reader (Biotek, USA). The MTT assay was also performed with the cells not being incubated with the nanostructures, and their viability was taken as 100%. The viabilities of the cells incubated with the nanostructures were obtained by comparing with those of the cells not being incubated with the nanostructures.

Apo-ONE homogeneous caspase-3 assay

Caspase 3 is activated in apoptosis (or programmed cell death). The active caspases show specificity for cleavage at the C-terminal side of the aspartate residue of the sequence DEVD (Asp-Glu-Val-Asp) that disable key homeostatic and repair enzymes and bring about systematic structural disassembly of dying cells. The luminogenic caspase 3 substrate containing tetrapeptide sequence DEVD was used for caspase 3 cleavage and generation of the luminescent signal based on the standard protocol (Promega, Madison, WI). For evaluating the activity of the caspase of the cell upon the NIR photothermal therapy, cells were seeded into 96-well plates (~1×10^5 cells $well^{-1}$) and allowed to attach for 24 h. After incubated with the aptamer-Ag-Au nanostructures for 30 min and irradiated at 0.20 W cm^{-2} for various

time (0-60 min), 100 μL of Caspase-Glo3/7 reagent (Promega) was added to each well, followed by incubation at room temperature for 30 min, the caspase 3/7 activity was evaluated by recording the luminescence of each sample using a microplate reader (Biotek, USA).

CytoTox-ONE homogeneous membrane integrity assay

The CytoTOx-ONE assay is a rapid, fluorescent measure of the release of lactase dehydrogenase (LDH) from cells with a damaged membrane. LDH released into the culture medium is measured with an enzymatic assay that results in the conversion of resazurin to resorufin. The reaction is performed directly in a homogeneous format in assay wells. Cells (~1×10^5 cells $well^{-1}$) were placed in 96-well plates in 100 μL of RPMI 1640 medium. After incubated with the aptamer-Ag-Au nanostructures for 30 min and irradiated at 0.20 W cm^{-2} for 60 min, the plates were equilibrated at room temperature for 30 min, 100 μL of CytoTox-ONE reagent (Sigma) was added to each well and the plates were incubated for 10 min at room temperature. The fluorescence signal at 590 nm was recorded with an excitation source of 560 nm on a Synergy 2 microplate reader (Biotek, USA). LDH release was expressed relative to the basal LDH release from untreated control cells.

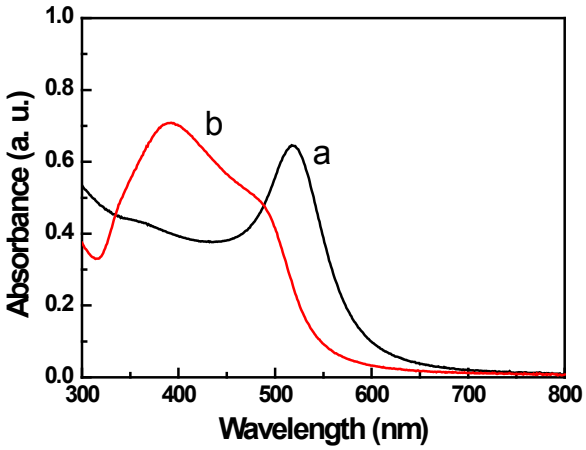

Fig. S1 UV-vis absorption spectra of (a) Au core (~20 nm) and (b) Ag-Au shell-core nanostructures (~28–30 nm).

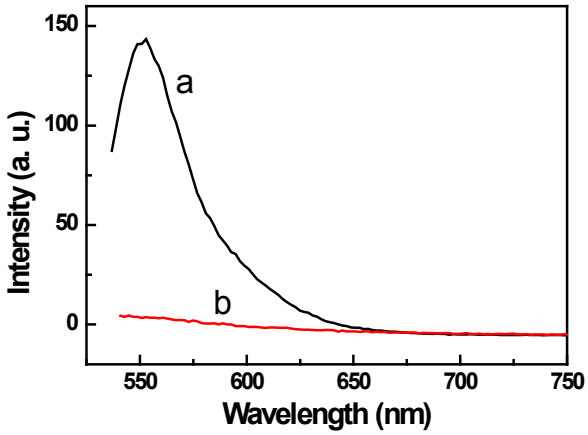

Fig. S2 Fluorescence of the free Rh6G (0.01 μM, a) and supernatant of the Rh6G-labeled Ag-Au nanostructures after centrifugation (b).

To check the adsorption stability on the Ag-Au nanostructures, we dispersed the Rh6G-labeled Ag-Au nanostructures (50 μg mL^{-1}) into water (1 mL) and stirred for 2 h at 250 rpm, and then the suspension was centrifuged at 10000 rpm. The supernatant was collected and its fluorescence spectrum was recorded. As shown in curve (b), no fluorescence signal of Rh6G was detected, indicating that almost no Rh6G molecule was desorbed from the surface of Ag-Au nanostructures. These results demonstrate that the adsorption of Rh6G on the Ag-Au nanostructures is stable.

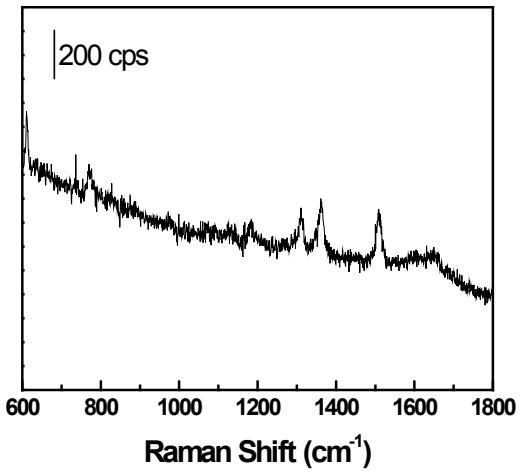

Fig. S3 Raman spectrum of Rh6G bulk solution on mica substrate (10 μL of 1 mM Rh6G solution was dispersed on the clean mica substrate).

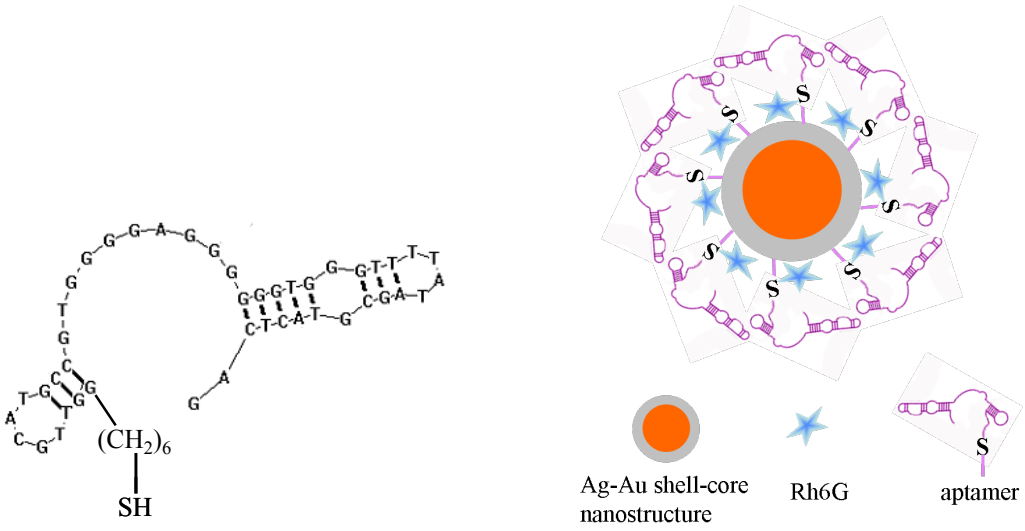

(A) (B)

Fig. S4 (A) The configuration of the aptamer obtained by the simulation using the RNA Structure (Version 5.2). (B) Illustration of the configuration of the Rh6G-labeled aptamer-Ag-Au shell-core nanostructures.

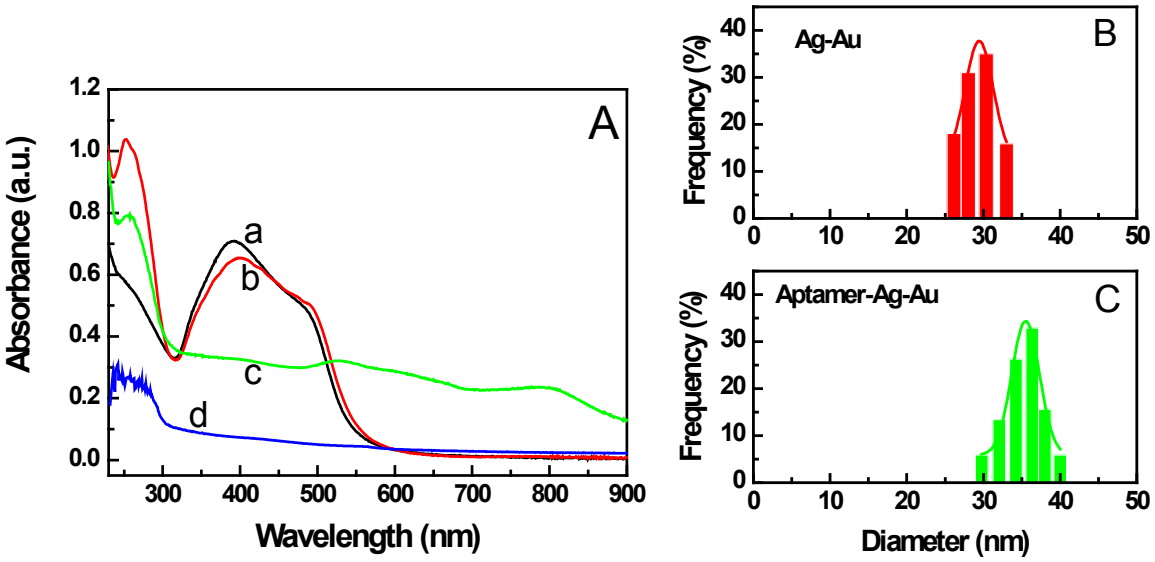

Fig. S5 (A) UV–vis spectra of (a) Ag-Au, (b) aptamer-Ag-Au nanostructures, and (c) the aptamer-Ag-Au nanostructures bound on the surface of the A549 cells. Curve d is the UV-vis spectrum of the A549 cells in PBS. (B) and (C) DLS size distribution of the Ag-Au (B) and aptamer-Ag-Au nanostructures (C).

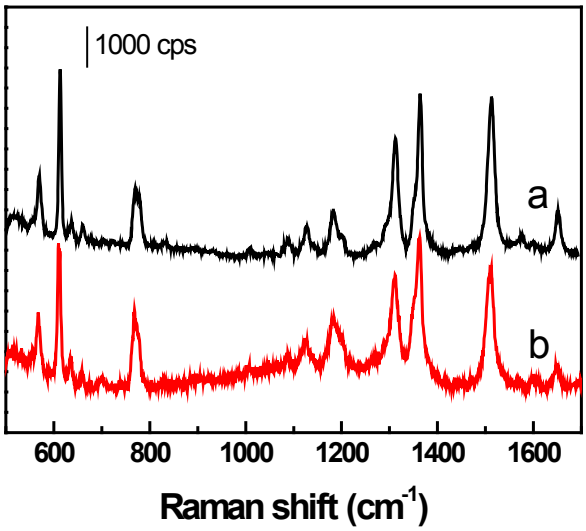

Fig. S6 SERS spectra of Rh6G labeled at the surface of Ag-Au nanostructures before (a) and after (b) the nanostructures were conjugated with the aptamer.

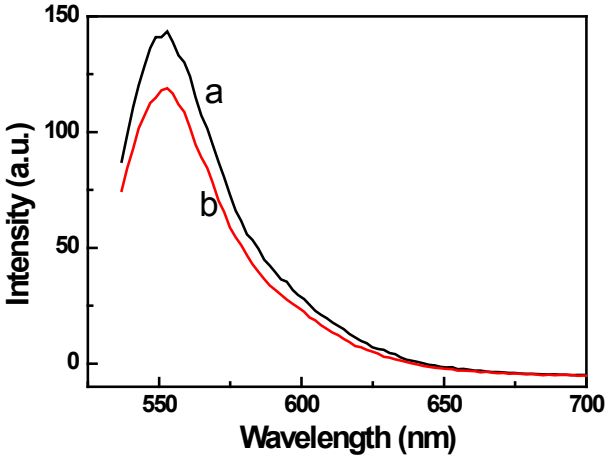

Fig. S7 Fluorescence spectra of free Rh6G (0.01 μM, a) and Rh6G-labeled aptamer-Ag-Au nanostructures (50 μg mL^{-1}, b).

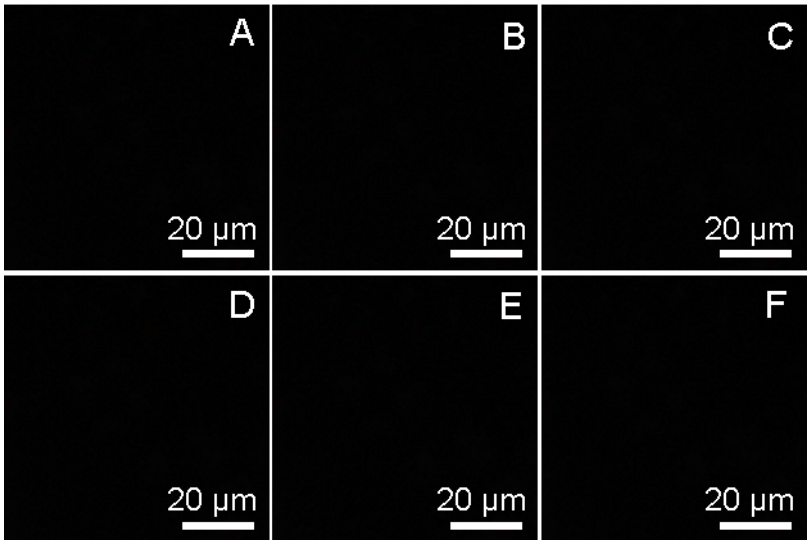

Fig. S8 Fluorescence images of NCI-H157 (A), NCI-H520 (B), NCI-H1299 (C), NCI-H446 (D), HeLa (E), and MCF-7 cells (F) with binding of the Rh6G-labeled aptamer-Ag-Au nanostructures. Before recording the images, the cells were washed thrice with PBS.

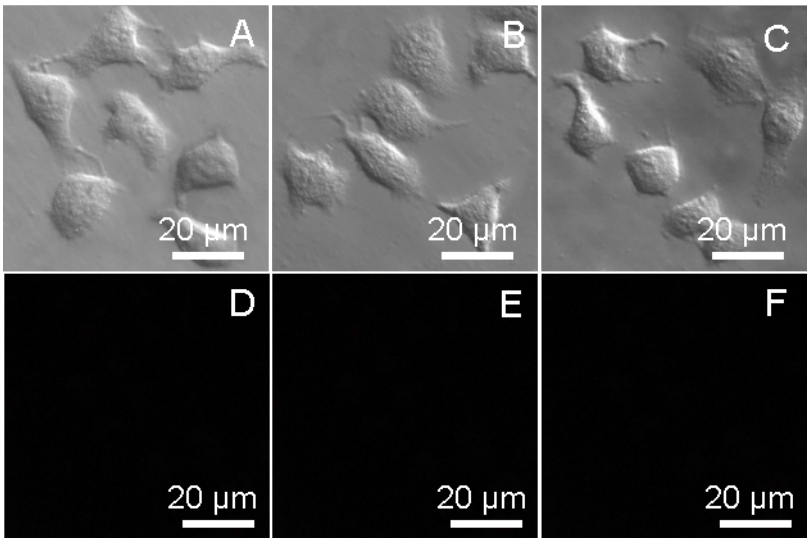

Fig. S9 DIC (A, B, and C) and fluorescence (D, E, and F) images of A549 cells with binding of the Rh6G-labeled aptamer-Ag-Au nanostructures, which were grown on the three-base mismatched DNA (A, D), on sgc8 aptamer (B, E), and on TDO5 aptamer chain (C, F), respectively. Before recording the images, the cells were washed thrice with PBS.

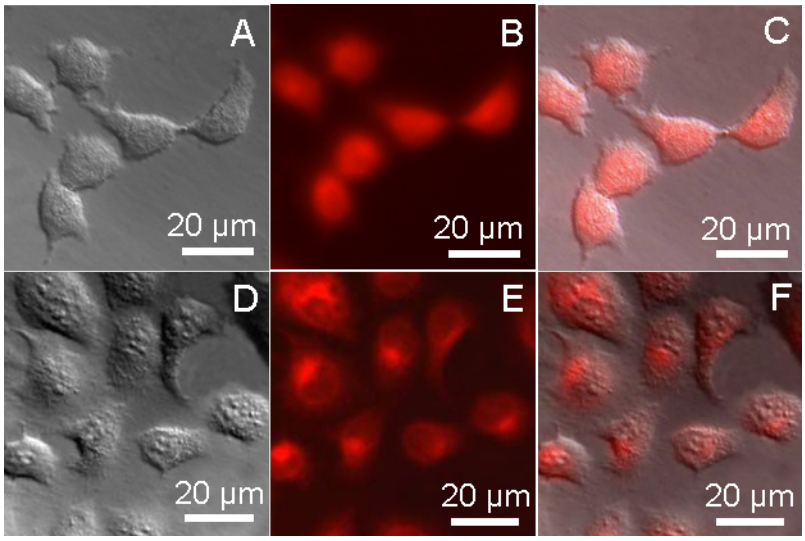

Fig. S10 Fluorescence (A, B), DIC (B, E), and their superimposed (C, F) images of A549 cells after incubated with free Rh6G (A-C) and with Rh6G-labeled aptamer-Ag-Au nanostructures, respectively. Before recording the images, the cells were washed thrice with PBS.

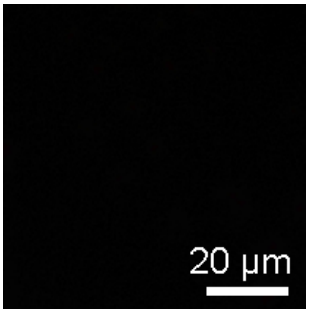

Fig. S11 Fluorescence images of A459 cells with binding of the Rh6G-labeled Ag-Au nanostructures (without conjugation of the aptamer). Before recording the images, the cells were washed thrice with PBS.

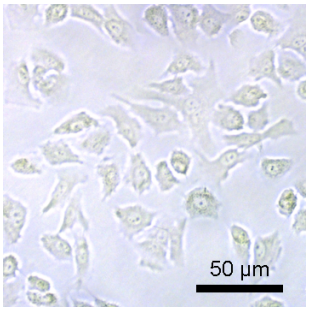

Fig. S12 Bright-field microscopic images of A549 cells (without incubating with the Rh6G-labeled aptamer-Ag-Au nanostructures) after irradiated for 60 min at power densities of 0.20 W cm^{-2}. The images were recorded after stained with trypan blue.

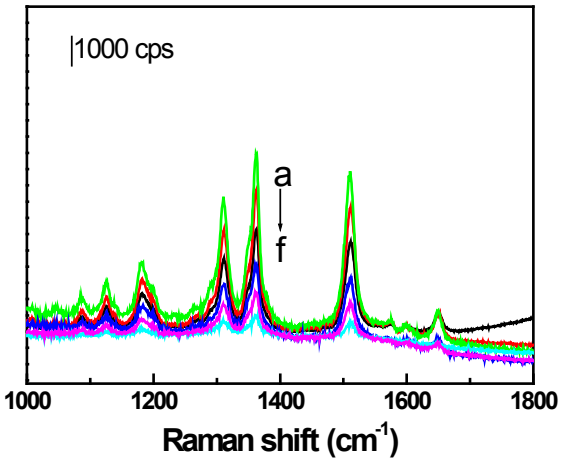

Fig. S13 SERS spectra A549 cells bound with Rh6G-labeled aptamer-Ag-Au nanostructures after irradiated at 808 nm with the irradiation power density of 0.20 W cm^{-1} for (a) 0, (b) 5, (c) 15, (d) 30, (e) 45, and (f) 60 min, respectively.

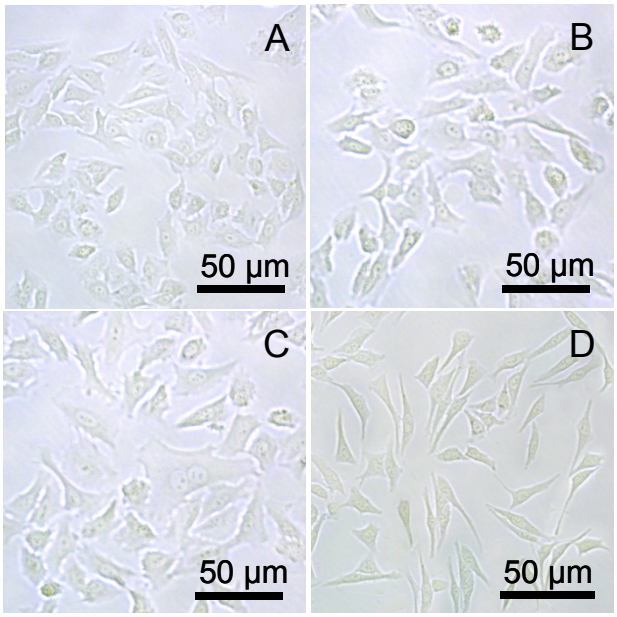

Fig. S14 Bright-field microscopic images of NCI-H157 (A), NCI-H446 (B), MCF-7 (C), and HeLa cells (D) cells after being incubated with the Rh6G-labeled aptamer-Ag-Au nanostructures and irradiated for 60 min at power densities of 0.20 W cm^{-2}. The images were recorded after stained with trypan blue.